

Electronic structure properties and BCS superconductivity in β -pyrochlore oxides: KOs_2O_6

R. Saniz, J. E. Medvedeva, Lin-Hui Ye, T. Shishidou,* and A. J. Freeman

Department of Physics and Astronomy, Northwestern University, Evanston, Illinois 60208-3112, USA

(Received 22 June 2004; revised manuscript received 11 August 2004; published 29 September 2004)

We report a first-principles density-functional calculation of the electronic structure and properties of the recently discovered superconducting β -pyrochlore oxide KOs_2O_6 . We find that the electronic structure near the Fermi energy E_F is dominated by strongly hybridized Os $5d$ and O $2p$ states. A van Hove singularity very close to E_F leads to a relatively large density of states at E_F , and the Fermi surface exhibits strong nesting along several directions. These features could provide the scattering processes leading to the observed anomalous temperature dependence of the resistivity and to the rather large specific-heat mass enhancement we obtain from the calculated density of states and the observed specific-heat coefficient. An estimate of T_c within the framework of the BCS theory of superconductivity taking into account the possible effects of spin fluctuations arising from nesting yields the experimental value.

DOI: 10.1103/PhysRevB.70.100505

PACS number(s): 74.20.Dd, 74.25.Jb, 71.20.Be

Transition-metal (TM) oxides are of intrinsic interest in physics because of the very rich phenomenology they exhibit due to electron correlations, ranging from metal-insulator transitions to colossal magnetoresistance and high critical temperature superconductivity. TM oxide compounds with the pyrochlore structure have long been studied and have found many applications thanks to their diverse electronic properties,¹ but it is not until recently that superconductivity was found in one such material, namely $\text{Cd}_2\text{Re}_2\text{O}_7$.^{2,3} Although its superconducting critical temperature turned out to be low ($T_c \approx 1$ K), it was an important discovery because it opened research in this area to a new class of materials. Very recently, superconductivity was reported in KOs_2O_6 ,^{4,5} a so-called β -pyrochlore, with a T_c of 9.6 K. More reports of superconductivity in the same family of compounds have followed at a rapid pace, with superconductivity being observed in RbOs_2O_6 ($T_c=6.3$ K) (Refs. 6 and 8) and in CsOs_2O_6 ($T_c=3.3$ K),¹⁰ adding to the interest in these materials.

The discovery of superconductivity in the β -pyrochlores raises of course, the question of the underlying mechanism. While the mechanism in $\text{Cd}_2\text{Re}_2\text{O}_7$, an α -pyrochlore,¹⁰ can be understood within the weak-coupling Bardeen, Cooper, and Schrieffer (BCS) theory of superconductivity,¹¹ Hiroi and co-workers have suggested⁵ from the outset that KOs_2O_6 is an unconventional superconductor, with the pairing mediated by spin fluctuations.⁷ On the other hand, Brühwiler and co-workers suggested⁸ that RbOs_2O_6 could be a conventional BCS-type superconductor, and recent pressure effects measurements appear to bring further support to their conclusions.⁹ Given the close similarity between these two compounds, it seems unlikely that their superconductivity has a different origin. Clearly, a careful study of the electronic structure of these materials may shed light on the superconductivity mechanism.

In this work, we focus on KOs_2O_6 and carry out a self-consistent first-principles density-functional calculation of its electronic structure, using a parallelized implementation¹² of the full-potential linearized augmented plane-wave (FLAPW) method.¹³ Our calculations are made within the

Perdew, Burke, and Ernzerhof generalized gradient approximation¹⁴ (GGA) to the exchange-correlation potential and include the spin-orbit coupling (SOC) term in the Hamiltonian. Our results show that the electronic structure near the Fermi energy (E_F) is dominated by strongly hybridized Os $5d$ and O $2p$ states. There is a van Hove singularity (vHS) very close to E_F , leading to a relatively large density of states (DOS) at E_F , and the Fermi surface shows strong nesting along several directions. These features could provide the scattering processes leading to the reported^{4,5} anomalous temperature dependence of the resistivity above T_c , and to the rather large specific-heat mass enhancement we obtain from the calculated DOS and the measured low-temperature specific-heat coefficient.⁵ We estimate the T_c within the BCS framework and are able to obtain the experimental value if we take into account the possible effects of spin fluctuations arising from nesting.

KOs_2O_6 crystallizes in a cubic structure with space group $Fd\bar{3}m$, and has 18 atoms per unit cell: two K ($8b$), four Os ($16c$), and twelve O ($48f$).⁴ The structure has an internal parameter x that fixes the position of the oxygen atoms. The experimental lattice constant recently given by Yonezawa and co-workers is $a=10.101$ Å,⁵ but no value for the x parameter has yet been reported. The muffin-tin radii used in our calculations for K, Os, and O are 5.29 Å, 4.16 Å, and 2.46 Å, respectively. Angular momenta up to $l=8$ were used for both the wave functions and the charge density in the muffin-tin spheres, and the irreducible part of the Brillouin zone was sampled with a uniform mesh of 120 \mathbf{k} points. We have optimized variationally both the lattice constant and the internal parameter, obtaining $a=10.298$ Å, which differs by 1.95% from the experimental value, and $x=0.316$. The latter can be compared with the value of $x=0.315$ recently reported for the related superconducting pyrochlore RbOs_2O_6 .⁸ Each Os atom is octahedrally coordinated by six O atoms, with O-Os-O angles of 88.66° and 91.34° (compare with 88.85° and 91.15°, respectively, for RbOs_2O_6 , reported in Ref. 8). Unlike the perovskite superconductors, in the pyrochlore oxides the TM-O octahedra are not distorted. The Os-O distance we find is 1.94 Å (compare with, for example, the

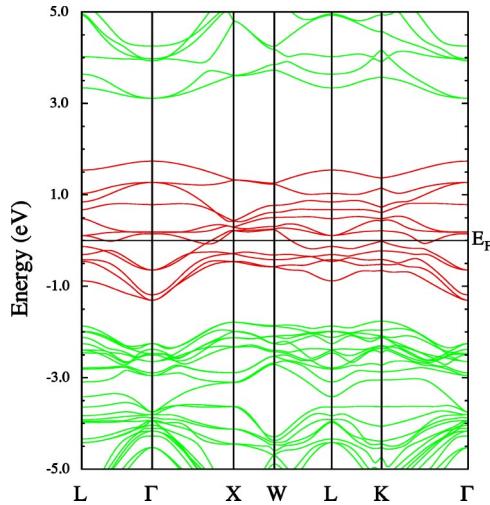


FIG. 1. (Color online) Electronic band structure of KOs_2O_6 . The 12 bands around E_F arise from Os $5d$ and O $2p$ states. A saddle point near the center of the ΓL line causes a vHS very close to E_F .

calculated^{17,18} Ru-O distances of 1.93 Å and 2.061 Å in Sr_2RuO_4). In KOs_2O_6 , the pyrochlore lattice is formed by highly interconnected Os-O staggered chains, resulting in corner sharing tetrahedra, with the Os ions occupying the vertices. In Ref. 8, it is suggested that in the β -pyrochlore oxides, the TM-O-TM angle plays a role in defining the superconducting properties, with smaller angles favoring higher critical temperatures. For KOs_2O_6 , we find an Os-O-Os angle of 139.16° , which is indeed smaller than the reported angle of 139.4° for RbOs_2O_6 .⁸ Experimental information regarding CsOs_2O_6 is currently insufficient for a comparison with this material.

The calculated energy bands along high symmetry directions in \mathbf{k} space, within 5 eV from E_F , are shown in Fig. 1. There is a manifold of 12 states in the vicinity of E_F , with a bandwidth of 3 eV, separated by relatively large energy gaps above and below. Note that in line with previous findings in the osmates, such a bandwidth classifies KOs_2O_6 as a system with moderately correlated electrons.^{15,16} Two bands cross E_F : the lower band, cutting the ΓX and $W L$ lines, gives rise to a holelike Fermi-surface sheet in the form of a tubular network; the upper band crosses E_F twice within the first Brillouin zone (cf. the ΓL , ΓX , and ΓK lines), giving rise to two Fermi-surface sheets. As will be illustrated below, this results in an electronlike closed shell centered at the Γ point. Of importance is the existence of a vHS very close to E_F , caused by a saddle point between the two sheets at ~ 0.015 eV below E_F , near the middle of the ΓL line.

The character of the bands near E_F is further analyzed by examining the DOS. The total DOS, shown in Fig. 2(a), exhibits a peak very close to E_F , due to the vHS mentioned above. We point out that a precursor of the peak is already present in a calculation without including SOC, at a slightly lower energy; the inclusion of SOC splits this peak, causes the saddle point, and pushes the higher peak closer to E_F . The l -projected partial DOS were evaluated by integrating the appropriate charge inside the muffin-tin spheres. In Fig. 2(b) we show the partial DOS of the O $2p$ and Os $5d$ states,

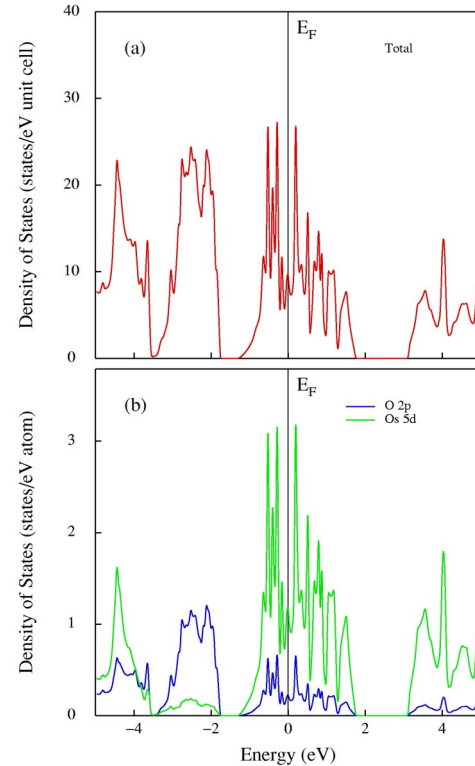


FIG. 2. (Color online) Electronic density of states of KOs_2O_6 . (a) Total DOS, showing a sharp peak very close to E_F . (b) Projected DOS of the O $2p$ and Os $5d$ states.

which are by far the dominant states in the energy range shown. As in previously studied oxide superconductors,^{15–18} the TM and O states are strongly hybridized near E_F . The orbital character of the states near E_F is Os $d\epsilon(xy, yz, zx)$ and O $p\pi$. This is clearly shown in Fig. 3, which presents a contour plot of the charge density in the $(1\bar{1}0)$ plane for states lying within 0.027 eV below E_F .¹⁹

An important finding is that the Fermi surface shows strong nesting, in particular the shell-like sheets. Contour plots of the eigenenergies for the corresponding band along two different planes centered at the Γ point are given in Fig. 4. Figure 4(a) shows the contour plot for \mathbf{k} in the $X\Gamma X$ plane, with strong nesting occurring for $k \approx 0.44\pi/a$ and $k \approx 0.624\pi/a$ along the ΓK directions. Similarly, Fig. 4(b) shows a contour plot for \mathbf{k} in the $X\Gamma K$ plane, also showing strong nesting, in particular for $k \approx 0.644\pi/a$ along ΓL directions.

Consider further some of the properties deduced from the electronic structure in relation to experiment. Firstly, the DOS at E_F is relatively high, $N(E_F) = 9.8$ states/eV unit cell, yielding a Sommerfeld electronic specific-heat coefficient $\gamma = 5.78$ mJ/K² mol Os. This is much lower than the experimental value of 19 mJ/K² mol Os,⁵ a result based on an estimation of the specific heat jump at T_c and the BCS weak-coupling relation $\Delta C/\gamma T_c = 1.43$. Thus, we find a very large specific-heat mass enhancement $\gamma_{\text{exp}}/\gamma_{\text{band}} \approx 3.3$, though it is still smaller than that of, e.g., Sr_2RuO_4 , found to be 3.8 or more.^{17,18} The above mass enhancement represents a rather high coupling constant, $\lambda = 2.3$. Given the relatively low T_c

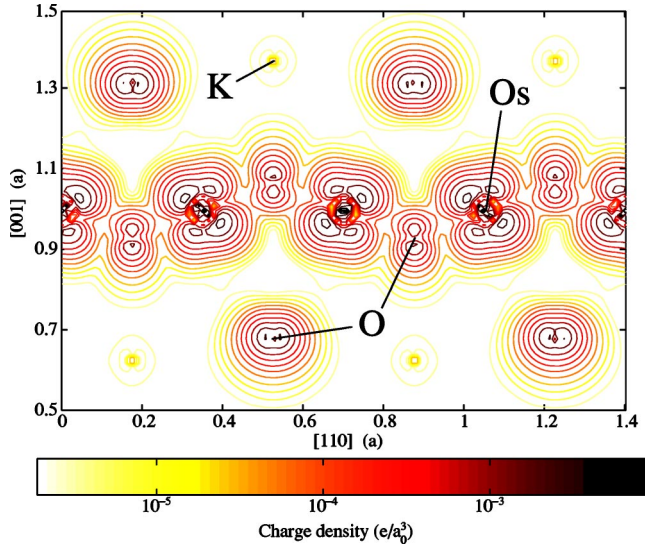


FIG. 3. (Color online) Contour plot of the charge density in the $(1\bar{1}0)$ plane for states lying within 0.027 eV below E_F . A staggered Os-O chain is clearly seen. The other O ions in the plot belong to chains traversing the $(1\bar{1}0)$ plane. As expected, the charge around the K ions is extremely weak.

of KOs_2O_6 , it appears that, besides the electron-phonon, contribution, there is a very important electronic many-body contribution to the specific-heat mass enhancement. Interestingly, Hiroi and co-workers noted in particular the unusual behavior of the measured resistivity as a function of temperature.^{4,5} Single-crystal data are greatly desirable to advance further in this direction. Let us just point out here that, under appropriate conditions, deviations from conventional Fermi-liquid behavior in two-dimensional systems can be caused by both vHS's near E_F and by Fermi-surface nesting,^{20,21} due to the increased phase space available for electron-electron scattering.²²

From the measured $T_c=9.6$ K, and using $\Delta=1.76k_B T_c$, the superconducting gap is calculated to be $\Delta=1.456$ meV. A calculation of the average Fermi velocity then allows us to readily estimate the BCS-Pippard coherence length $\xi_0=\hbar\langle v_F\rangle/\pi\Delta$. We find $\langle v_F\rangle=1.47\times 10^7$ cm/s, which yields $\xi_0=212$ Å. This is an order of magnitude larger than the reported Ginzburg-Landau coherence length $\xi=30$ Å, obtained from the estimated upper critical field H_{c2} .^{5,23} Thus, the so-called dirty limit would apply. Indeed, writing $\xi^{-1}=\xi_0^{-1}+l^{-1}$, with l the mean free path, yields an estimated value of $l=35$ Å. This relatively short value suggests again that strong scattering processes play an important role in the electronic properties of this material.

We estimate the McMillan-Hopfield^{24,25} electron-phonon coupling constant λ_{ep} , for which the constituent-weighted average can be written $\lambda_{ep}=\sum_i w_i \eta_i/M_i\langle\omega^2\rangle$.²⁶ The spherically averaged Hopfield parameter for each atom type, η_i , calculated in the crude rigid-muffin-tin approximation, is²⁷

$$\eta_i = 2N_i(E_F) \sum_l (l+1) M_{i,l+1}^2 \frac{f_i f_{l+1}}{(2l+1)(2l+3)}, \quad (1)$$

where $f_i=N_i(E_F)/N_i(E_F)$ is a relative partial DOS and $M_{i,l+1}=-\phi_i\phi_{i+1}[(D_i-l)(D_{i+1}+l+2)+(E_F-V_i)R_i^2]$ is an

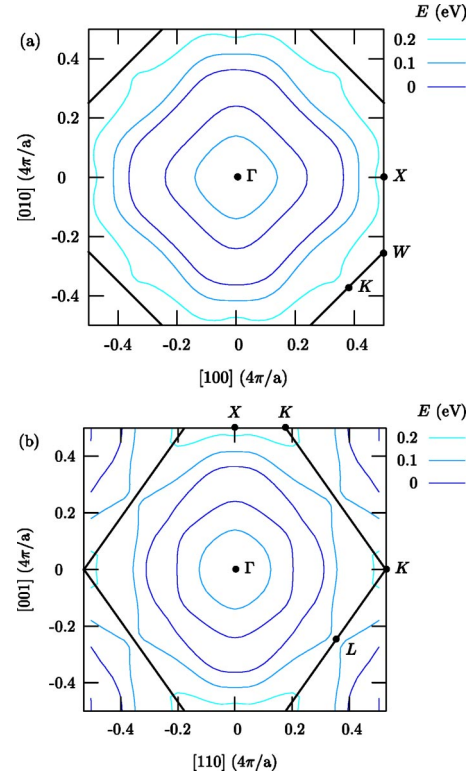


FIG. 4. (Color online) Contour plots of the upper band crossing E_F (cf. Fig. 1). The thick lines indicate the first Brillouin zone boundaries; $E=0$ corresponds to E_F . (a) Plot for $\mathbf{k}\in X\Gamma X$ plane. Extensive nesting occurs for $\mathbf{k}\parallel\Gamma K$, with $k\approx 0.4$ and 0.62 $4\pi/a$. (b) Plot for $\mathbf{k}\in\Gamma X K$ plane. Strong nesting occurs, e.g., for $\mathbf{k}\parallel\Gamma L$, with $k\approx 0.64$ $4\pi/a$.

electron-phonon matrix element.²⁸ In the latter, the logarithmic derivatives (D_i) and the partial-wave amplitudes (ϕ_i) are evaluated at E_F and at the muffin-tin radius (R_i) ; V_i is the one-electron potential at R_i . The average phonon frequency can be estimated by $\langle\omega^2\rangle^{1/2}=0.69\Theta_D$. There is currently no reported Θ_D for KOs_2O_6 , but Brühwiler and co-workers did such measurements for RbOs_2O_6 .⁸ Under the assumption that the values of Θ_D fall in the same range for both materials, we take $\Theta_D=240$ K, and obtain $\lambda_{ep}=1.1$. As expected, this value is well below the total λ obtained from the specific-heat mass enhancement discussed above.

To estimate T_c ,²⁹ we use the Allen and Dynes modification of the McMillan equation,^{24,30} including an effective electron-spin interaction coupling constant μ_{sp} ,³¹ i.e.,

$$T_c = \frac{\langle\omega^2\rangle^{1/2}}{1.2} \exp\left[-\frac{1.04(1+\lambda_{ep}+\mu_{sp})}{\lambda_{ep}-(\mu^*+\mu_{sp})(1+0.62\lambda_{ep})}\right]. \quad (2)$$

The so-called Coulomb pseudopotential μ^* can be estimated from the DOS at E_F ,³¹ and in our case is $\mu^*=0.09$. On the other hand, there is no simple expression for μ_{sp} . If $\mu_{sp}=0$ we find $T_c\approx 14$ K. A coupling constant $\mu_{sp}=0.06$,³² reflecting important spin fluctuations, would yield the experimental value $T_c=9.6$ K. As an estimation, from our DOS we have calculated the Pauli paramagnetic susceptibility, finding $\chi_{\text{band}}=1.58\times 10^{-4}$ cm³/mol. From Ref. 5, we estimate the

experimental value at $T=0$ to be $\chi_{\text{exp}} \approx 4 \times 10^{-4} \text{ cm}^3/\text{mol}$, which yields an enhancement ratio $\chi_{\text{exp}}/\chi_{\text{band}}=2.53$.³³ Since we expect the orbital contributions to the susceptibility enhancement to be weak,³⁴ spin fluctuations may indeed play an important role in KOs_2O_6 , and the significant nesting of the Fermi surface could be a key factor in this respect. On the other hand, from our calculated results above, the Wilson ratio is $R_W=0.77$, which is indicative of the dominance of electron-phonon coupling over electron correlations. This

further favors a phonon-mediated pairing scenario over a spin fluctuations one.

We are grateful to O. Kontsevoi, M. Weinert, T. Jarlborg, J. Yu, J. B. Ketterson, and J. A. Sauls for helpful discussions. This work was supported by the Department of Energy (under Grant No. DE-FG02-88ER 45372/A021 and a computer time grant at the National Energy Research Scientific Computing Center).

*Present address: Department of Quantum Matter, ADSM, Hiroshima University, Higashihiroshima 739-8530, Japan.

¹M. A. Subramanian, G. Aravamudan, and G. V. S. Rao, *Prog. Solid State Chem.* **15**, 55 (1983).

²M. Hanawa, Y. Muraoka, T. Tayama, T. Sakakibara, J. Yamaura, and Z. Hiroi, *Phys. Rev. Lett.* **87**, 187001 (2001).

³H. Sakai, K. Yoshimura, H. Ohno, H. Kato, S. Kambe, R. E. Walsted, T. D. Matsuda, Y. Haga, and Y. Ōnuki, *J. Phys.: Condens. Matter* **13**, L785 (2001).

⁴S. Yonezawa, Y. Muraoka, Y. Matsushita, and Z. Hiroi, *J. Phys.: Condens. Matter* **16**, L9 (2004).

⁵Z. Hiroi, S. Yonezawa, and Y. Muraoka, *cond-mat/0402006v1*, (unpublished).

⁶S. Yonezawa, Y. Muraoka, Y. Matsushita, and Z. Hiroi, *J. Phys. Soc. Jpn.* **73**, 819 (2004).

⁷A. Koda, W. Higemoto, K. Ohishi, S. R. Saha, R. Kadono, S. Yonezawa, Y. Muraoka, and Z. Hiroi, *cond-mat/0402400* (unpublished).

⁸M. Brühwiler, S. M. Kazakov, N. D. Zhigadlo, J. Karpinski, and B. Batlogg, *Phys. Rev. B* **70**, 020503(R) (2004).

⁹R. Khasanov, D. G. Eshchenko, J. Karpinski, S. M. Kazakov, N. D. Zhigadlo, R. Brüttsch, D. Gavillet, and H. Keller, *cond-mat/0404542* (unpublished).

¹⁰S. Yonezawa, Y. Muraoka, and Z. Hiroi, *J. Phys. Soc. Jpn.* **73**, 1655 (2004).

¹¹Z. Hiroi and M. Hanawa, *J. Phys. Chem. Solids* **63**, 1021 (2002).

¹²T. Shishidou, L.-H. Ye, M. Weinert, and A. J. Freeman (unpublished).

¹³E. Wimmer, H. Krakauer, M. Weinert, and A. J. Freeman, *Phys. Rev. B* **24**, 864 (1981); M. Weinert, E. Wimmer, and A. J. Freeman, *ibid.* **26**, 4571 (1982); H. J. F. Jansen and A. J. Freeman, *ibid.* **30**, 561 (1984).

¹⁴J. P. Perdew, K. Burke, and M. Ernzerhof, *Phys. Rev. Lett.* **77**, 3865 (1996).

¹⁵D. Mandrus, J. R. Thompson, R. Gaal, L. Forro, J. C. Bryan, B. C. Chakoumakos, L. M. Woods, B. C. Sales, R. S. Fishman, and V. Keppens, *Phys. Rev. B* **63**, 195104 (2001).

¹⁶D. J. Singh, P. Blaha, K. Schwarz, and J. O. Sofo, *Phys. Rev. B* **65**, 155109 (2002).

¹⁷T. Oguchi, *Phys. Rev. B* **51**, 1385 (1995).

¹⁸D. J. Singh, *Phys. Rev. B* **52**, 1358 (1995).

¹⁹This energy corresponds to 313 K, which is of the order of a typical Θ_D in metallic pyrochlores; see Ref. 8.

²⁰D. M. Newns, C. C. Tsuei, R. P. Huebener, P. J. M. van Bentum, P. C. Pattnaik, and C. C. Chi, *Phys. Rev. Lett.* **73**, 1695 (1994).

²¹A. Virosztek and J. Ruvalds, *Phys. Rev. B* **42**, 4064 (1990).

²²Moreover, disorder and/or impurities can play a critical role in this respect, as shown by A. Rosch, *Phys. Rev. Lett.* **82**, 4280 (1999).

²³We point out that although the estimated H_{c2} for KOs_2O_6 is high (38.3 T) and more than twice its Chandrasekhar-Clogston limit, those figures are not without precedent among BCS superconductors, being close to those of several ternary molybdenum chalcogenides; see M. Decroux and Ø. Fischer, in *Superconductivity in Ternary Compounds*, edited by M. B. Maple and Ø. Fischer (Springer-Verlag, Berlin, 1982). On the other hand, our results suggest that KOs_2O_6 is a strong-coupling superconductor, so some figures in Ref. 5 may require revision; see D. Rainer and G. Bergmann, *J. Low Temp. Phys.* **14**, 501 (1974).

²⁴W. L. McMillan, *Phys. Rev.* **167**, 331 (1968).

²⁵J. J. Hopfield, *Phys. Rev.* **186**, 443 (1969).

²⁶H. G. Salunke, R. Mittal, G. P. Das, and S. L. Chaplot, *J. Phys.: Condens. Matter* **9**, 10137 (1997).

²⁷H. L. Skriver and I. Mertig, *Phys. Rev. B* **32**, 4431 (1985).

²⁸Since $\eta_i \propto N_i(E_F)$, the relevance of potassium to λ_{ep} is indirect, mainly through its role in the determination of the structural parameters of the compound.

²⁹A more rigorous estimation of λ and of T_c may require a more elaborate approach than the one adopted here, due to the peak in the DOS very close to E_F . See, e.g., E. Cappelluti and L. Pietronero, *Phys. Rev. B* **53**, 932 (1996).

³⁰P. B. Allen and R. C. Dynes, *Phys. Rev. B* **12**, 905 (1975).

³¹K. Bennemann and J. Garland, in *Superconductivity in d- and f-band metals*, edited by D. H. Douglass, AIP Conf. Proc. No. 4 (AIP, New York, 1972), p. 103.

³²In TMs, μ_{sp} is generally around ~ 0.05 ; see Ref. 31.

³³This is comparable to the values found in the case of $\text{Cd}_2\text{Re}_2\text{O}_7$; see Ref. 16.

³⁴It has been shown that in $4d$ TMs the enhancement of the van Vleck susceptibility—the leading contribution to the orbital susceptibility—is only around 10%. Furthermore, the van Vleck term decreases when going from the $3d$ to the $5d$ families. See H. Ebert, S. Mankovsky, H. Freyer, and M. Deng, *J. Phys.: Condens. Matter* **15**, S617 (2003).